JAPAN/USA Symposium on Flexible Automation – Volume 1
ASME 1992

49

BILATERAL IMPEDANCE CONTROL FOR TELEMANIPULATORS

C. L. Moore
Space Systems Engineering Branch
NASA Langley Research Center
Hampton, Virginia

H. Kazerooni
Department of Mechanical Engineering
University of California, Berkeley
Berkeley, California

Abstract

The research investigates a new method of control for telemanipulators called bilateral impedance control. This new method differs from previous approaches in that interaction forces are used as the communication signals between the master and slave robots. The main advantage of bilateral impedance control is that it permits the arbitrary specification of desired system performance characteristics. Performance can be described by a set of three independent parameters that relate the robot forces and positions. This set of parameters may include the force ratio, the position ratio, and the robot impedances. The system stability is analyzed with the Nyquist Criterion to obtain two conditions that are sufficient to guarantee closed-loop stability. This control architecture is implemented on a telemanipulator having seven degrees of freedom. The theoretical predictions for performance and stability are experimentally verified.

Introduction

A telerobotic system consists of a master robot that is manipulated by a human operator, and a slave robot that performs tasks at a remote location. The two robots are electronically coupled so that the slave robot moves in response to commands from the master robot. Figure 1 shows the elements of a telerobotic system. The slave robot is shown interacting with an environment. In this paper "environment" refers to the object that the slave robot moves or manipulate through space.

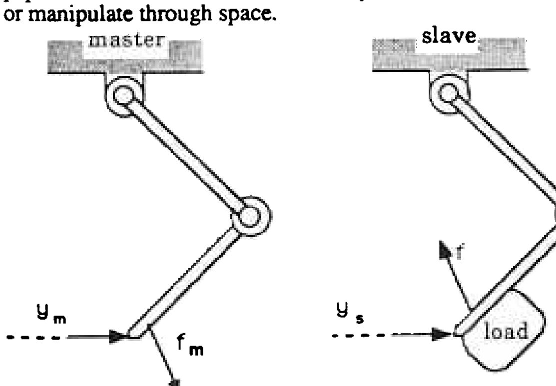

Figure 1: Elements of a Telerobotic System

Teleoperation is greatly enhanced if the forces acting on the slave robot are fed back to the operator. This gives the operator the feeling that she is manipulating the remote environment directly. Systems that provide force reflection from the environment are called bilateral because information travels in both directions between the master and slave.

In currently used telerobotic control methods, the slave robot is driven by position or velocity signals from the master robot [1-4]. Force reflection is implemented in several ways. The master robot may be back driven by position signals from the slave robot. The position error generated when the slave contacts the environment allows the operator to feel the interaction [2]. Alternately, the interaction force may be sensed directly by a force sensor on the slave, and the resulting force signal is used to back drive the master [2]. A comparison of common control methods is given in [5].

This paper proposes a new method of telerobotic control that is based solely on the exchange of force signals. The proposed control architecture has several advantages over previous approaches. It permits the arbitrary specification of desired system performance characteristics. The relationship between force and position can be modulated at both ends of the system to suit the requirements of the task. The master and slave robots can be stabilized independently without becoming involved in the overall system dynamics. Finally, the new control method allows the human to overcome the master robot's resistance to motion if it has high friction, inertia, or gear reduction.

Dynamic Models

The dynamic behavior of a telerobotic system results from the interaction of its components: the master and slave robots, the human, and the environment. Linear dynamic models will be developed separately for each of these components. The models will then be assembled to form a telerobotic control architecture that describes overall system behavior. A single-degree-of-freedom telerobotic system is discussed in this paper; the multivariable control technique is described in 12.

It is assumed that both robots are stabilized by independent, closed-loop position controllers that keep them stationary when the human is not interacting with the system. The stabilizing controllers may include velocity feedback, but closed-loop velocity control by itself cannot guarantee that the slave will always track the master motion.

The master robot position, y_m, is a function of two inputs: the mechanical power transferred from the human arm, and the electronic commands sent to the robot control system. The transfer function G_m represents the master robot's closed-loop control system, which incorporates the dynamics of the robot and its stabilizing compensator. The input to the master control system is the electronic command, u_m. The output is the master position, y_m. The transfer function S_m is the master sensitivity. It relates the force imposed on the master robot, f_m, to the master position, y_m. The sensitivity depends on the robot's mechanical characteristics, and on the gain of the stabilizing position controller. Equation (1) represents the master robot dynamic behavior in general form.

$$y_m = G_m u_m + S_m f_m \tag{1}$$

Since the master robot is in contact with the human, f_m is the force exerted by the human arm. Similarly, the dynamic behavior of the slave robot can be defined by

$$y_s = G_s u_s + S_s f_s \tag{2}$$

where f_s is the force imposed on the slave robot by the environment, and u_s is the electronic input command to the slave control system. The transfer functions G_s and S_s represent the slave robot's closed-loop control system and the slave sensitivity, respectively.

The human arm can be modeled as a non-ideal force control system [6]. The force exerted on the master robot by the human arm results from two inputs. The first input, u_h, is issued by the human central nervous system. The specific form of u_h is not known, other than it is the human thought deciding to impose a force on the robot. This unstructured representation implicitly accounts for the internal dynamics of muscle contraction, nerve conduction, and central nervous system processing. The second input is the motion of the master robot. The human arm sensitivity function, S_h, maps the master robot position, y_m, into the imposed force, f_m. The dynamic equation of the human arm is

$$f_m = u_h - S_h y_m \tag{3}$$

The minus sign indicates that the reaction force exerted on the robot by the human arm is opposite in direction to the robot motion.

The environmental dynamics can be represented by a transfer function E that relates the slave position, y_s, to the force imposed on the slave robot, f_s. For example, if the slave robot is pushing against a spring and damper, the environmental dynamics are $E(s) = (K + Cs)$ where K, C, and s are the stiffness, damping, and Laplace operator. If the slave robot is manuevering an object of mass M, the environmental dynamics are $E(s) = Ms^2$. A general expression for the total force imposed on the slave robot is

$$f_s = f_{ext} - E\, y_s \tag{4}$$

where f_{ext} is the resultant of all external forces on the environment. The environment is usually considered to be a passive element with no independent sources of energy. Thus, in most cases, it is assumed that $f_{ext} = 0$. The minus sign in Equation (4) indicates that the reaction force exerted on the robot by the environment is opposite in direction to the robot displacement.

Bilateral Impedance Control

The overall dynamic behavior of the telerobotic system can be represented by a block diagram in Figure 2. This block diagram is constructed by combining the dynamic equations for the master and slave robots, the human, and the environment (Equations 1-4). The matrix, H, is added to the system for control and operates on the interaction forces, f_m and f_s only.

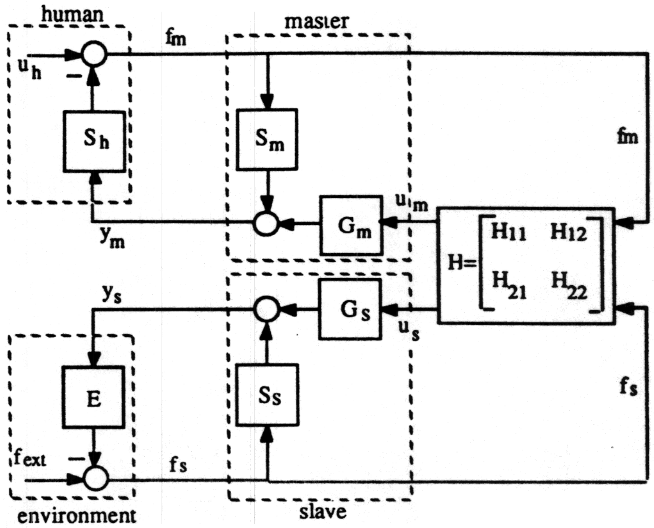

Figure 2: Bilateral Impedance Control Architecture

To see how the control method works, suppose that both the master and slave robots are initially at rest with no forces imposed on the system. Then there are no input commands to the robot control systems, and the stabilizing position controllers keep both robots stationary. Now, if the human decides to move her hand, u_h becomes nonzero, and the master robot starts to move. This motion is a result of the mechanical power transferred from the human to the master. Even though the force applied by the human may be very large, the master robot motion will be small if the sensitivity S_m is small. In other words, the human may not be strong enough to overcome the master robot's resistance to motion (impedance).

To increase the human's effective strength, the apparent sensitivity of the master robot is increased by measuring the interaction force, f_m, and using it as an input to the master control system. The interaction force is modified by the compensator H_{11}, which produces as its output the master input command, u_m. At this point, there are no restrictions placed on either the structure or size of the compensator. Note that $G_m H_{11}$ acts in parallel to S_m, and thus has the effect of changing the apparent sensitivity of the master robot. The master's apparent sensitivity can be increased by choosing a large gain for H_{11}. This is equivalent to reducing the master impedance.

The impedance of the slave robot is controlled in a similar manner to that of the master robot. The force imposed on the slave robot by the environment, f_s, is measured and used as an input command to the slave control system. The environmental interaction force is modified by the compensator H_{22}, which produces as its output the slave input command, u_s. This compensator generates compliance in the slave robot. Compliance is necessary for system stability, and it prevents the build up of large contact forces when the slave encounters a rigid surface [5].

The measured interaction forces f_m and f_s are also used as the communication signals between the master and the slave. The bilateral communication is regulated by the two compensators H_{12} and H_{21}. The master interaction force f_m is used to drive the slave robot after passing through the compensator H_{21}. This compensator transmits information in the forward direction from the master to the slave, and thus couples the motions of the two robots. The slave interaction force f_s is used to drive the master robot after passing through the compensator H_{12}. This compensator transmits information in the reverse direction from the slave to the master, and thus provides force reflection.

The compensators H_{11}, H_{12}, H_{21}, and H_{22} make up the elements of the matrix H. By proper selection of these four elements, the system designers can achieve desired performance characteristics. However, the designers do not have complete freedom in choosing the value of H. The closed-loop system of Figure 2 must remain stable for any chosen value of H.

The proposed control architecture is called bilateral impedance control because it establishes a relationship between force and position at both ends of the telerobotic system. The central difference between this new control method and previous architectures is that interaction forces are used as the communication signals between the master and slave. The flow of force signals within the system is regulated by the H matrix. This matrix permits the arbitrary specification of system performance.

Performance Parameters

The ideal performance of a telerobotic system can be expressed in many ways. One way is to strive for a completely transparent interface between the human operator and the environment. If such a system could be attained, the operator would experience the same sensations as if she were actually present at the remote location. This may not always be desirable, however. For example, suppose that the telerobotic system is used to maneuver a large, massive object through an arbitrary trajectory. Inertial, centrifugal, coriolis, and gravitational forces will be imposed on the slave. It seems reasonable to mask the dynamic behavior of the load through the design of appropriate controllers so that the human feels scaled-down values of these forces. In another example, suppose that the slave is holding a vibrating jack hammer. The objective is to filter the forces transferred to the master so that the human feels only the low frequency components [7]. These examples illustrate that in the most general case, it should be possible to specify any desired relationship between the master and slave forces.

In addition, it should be possible to specify a desired relationship between the master and slave positions. For example, the slave robot could perform small, precise motions in response to large, coarse motions of the master robot. This position scaling would have applications in microsurgery [7]. Thus, in general, it is necessary to shape the relationships between the forces and the positions at both ends of the system such that

$$f_s = R_f \, f_m \qquad (5)$$

$$y_s = R_y \, y_m \qquad (6)$$

where the transfer functions R_f and R_y represent the desired relationships.

The performance of the telerobotic system can be characterized by four state variables. These are the forces f_m and f_s, and the positions y_m and y_s. In Figure 3, the lines connecting the circled state variables represent possible relationships between them. Only three independent relationships are needed to relate the state variables. Two of these relationships are given by equations 5 and 6. A third relationship must be specified that relates either f_m and y_m, or f_s and y_s.[1] Choosing the relationship between the slave variables, the necessary third equation is

$$f_s = Z_s \, y_s \qquad (7)$$

where Z_s is the slave impedance.

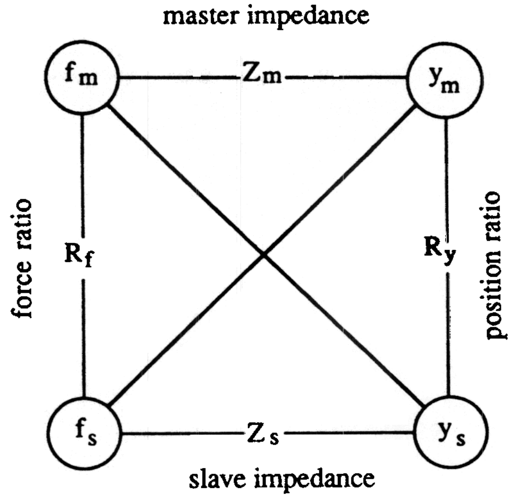

Figure 3: State Variable Relationships for a Telerobotic System

The three parameters R_f, R_y, and Z_s completely describe the system performance. These parameters are independent, and thus can be arbitrarily specified to achieve desired performance characteristics. Other sets of three parameters can also be used to describe system performance, as long as the parameters are independent. For example, Z_m, Z_s, and R_f constitute such a set.

The performance parameters are fundamentally related to the elements in the H matrix. To make this relationship apparent, the performance parameters are expressed in terms of the system variables G_m, G_s, S_m, S_s, S_h, and E. The following equations can be obtained from the block diagram of Figure 2:

$$R_f = \frac{-P_{21} E}{1 + P_{22} E} \qquad (8)$$

$$R_y = \frac{P_{21}}{P_{11} + \Delta P \; E} \qquad (9)$$

$$Z_m = \frac{1 + P_{22} E}{P_{11} + \Delta P \; E} \qquad (10)$$

$$Z_s = \frac{1 + P_{11} S_h}{P_{22} + \Delta P \; S_h} \quad \text{when } u_h = 0 \qquad (11)$$

where:

$$P_{11} = G_m H_{11} + S_m \qquad (12)$$

$$P_{12} = G_m H_{12} \qquad (13)$$

$$P_{21} = G_s H_{21} \qquad (14)$$

$$P_{22} = G_s H_{22} + S_s \qquad (15)$$

$$\Delta P = P_{11} P_{22} - P_{12} P_{21} \qquad (16)$$

It can be seen from equations (8) through (16) that the performance parameters depend on the relative magnitudes of the elements in H. If values are known for the system variables, the H matrix can be designed to achieve desired values for the performance parameters. The process of H matrix design will be illustrated by an example during experimental verification.

[1]While it is theoretically possible to specify a relationship between y_m and f_s, or between f_m and y_s, these relationships have no physical significance.

Stability

The arbitrary specification of desired performance characteristics may conflict with the requirements for system stability. In other words, there may be a trade-off between performance and stability. The Nyquist Criterion will be used to derive the conditions that are sufficient to guarantee closed-loop stability of linear systems with transfer function matrix operators. It will be shown that the stability conditions place limitations on possible structures for the H matrix.

The telerobotic control architecture must be reduced to an equivalent loop transfer function before the Nyquist Criterion can be applied [8]. Using matrix operators, the block diagram in Figure 2 can be rearranged to obtain the simplified block diagram shown in Figure 4. A single control loop has been formed by merging the separate control loops of the master and slave robots. Further simplification is possible by combining the G, H, and S matrices using the rules of block diagram algebra. Let the matrix P be defined such that

$$P = GH + S \qquad (17)$$

Note that the elements of P are given by equations (12) through (15). From the simplified block diagram, the equivalent loop transfer function of the telerobotic system is RP.

The Nyquist Criterion states that for closed-loop stability of a linear system, the equivalent loop transfer function must satisfy the following condition [8]:

$$\det[I + RP] \neq 0 \quad \text{for all } \omega \in [0, \infty] \qquad (18)$$

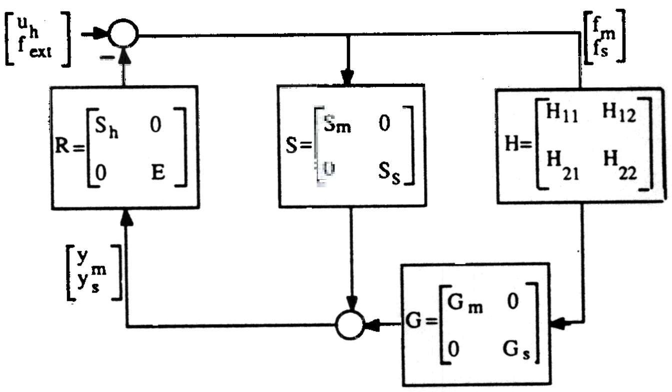

Figure 4: Simplified Block Diagram in Matrix Form

Substituting the elements of R and P into equation (18) for calculation of the determinant yields

$$S_h E \, \Delta P + S_h P_{11} + P_{22} E + 1 \neq 0 \quad \text{for all } \omega \in [0, \infty] \qquad (19)$$

For the system to be stable, the left hand side of equation (19) must not equal zero. If it is assumed that

$$S_h P_{11} + 1 \neq 0 \quad \text{for all } \omega \in [0, \infty] \qquad (20)$$

equation (19) can be written as

$$+\frac{E[S_h \Delta P + P_{22}]}{S_h P_{11} + 1} \neq 0 \quad \text{for all } \omega \in [0, \infty] \qquad (21)$$

A sufficient condition to insure the validity of equation (21) is

$$\left| \frac{E[S_h \Delta P + P_{22}]}{S_h P_{11} + 1} \right| < \qquad (22)$$

which implies that

$$\left| \frac{1 + S_h P_{11}}{P_{22} + S_h \Delta P} \right| > |E| \qquad (23)$$

This is the stability condition for constrained motion, which occurs when the slave robot is interacting with the environment. Comparing the left hand side of inequality (23) to equation (11), it can be seen that the stability condition is really a limitation on possible values of the slave impedance. That is, for stability

$$|Z_s| > |E| \qquad (24)$$

The slave impedance must be greater than the impedance of the environment. Since Z_s is a performance parameter that can be arbitrarily specified, it is usually possible to stabilize the system by selecting a sufficiently large value for the slave impedance. There is no conflict between performance and stability in this case. However, if the slave robot is in contact with a rigid surface, the slave impedance must be very large to stabilize the system. As $E \rightarrow \infty$, it is impossible to specify Z_s large enough such that stability of the system is guaranteed. Thus, there must be some initial compliancy in the environment for the system to be stable.

In deriving equation (21), it was assumed that inequality (20) must be true. A sufficient condition to insure the validity of equation (20) is

$$|S_h P_{11}| < 1 \qquad (25)$$

which implies that

$$|P_{11}| < \left| \frac{1}{S_h} \right| \qquad (26)$$

This is the stability condition for unconstrained motion. When the slave robot is moving freely through space, (i.e., E = 0), equation (10) for the master impedance becomes

$$Z_m = \frac{1}{P_{11}} \qquad (27)$$

Comparing equation (27) with inequality (26), it can be seen that the stability condition is really a limitation on possible values of the master impedance. That is, for stability

$$|Z_m| > |S_h| \quad \text{when } E = 0 \qquad (28)$$

The master impedance must be greater than the impedance of the human arm. Since Z_m is a performance parameter that can be arbitrarily specified, there is no conflict between performance and stability in most cases. However, if the human grips the master robot tightly, the master impedance must be very large to stabilize the system. As $S_h \rightarrow \infty$, it is impossible to specify Z_m large enough such that stability of the system is guaranteed. Thus, there must be some initial compliancy in the human arm for the system to be stable.

Experimental Verification

The theoretical predictions for performance and stability were experimentally verified on the seven-degree-of freedom NASA Laboratory Telerobotic Manipulator (Figure 5). A detailed description on this telerobotic system can be found in references

[10] and [11]. Due to the large inertia of the robots, the system is maneuvered at low speeds and the static values of the system variables are sufficient to charaterize the telerobotic system. It was found that G_m = 0.0117 rad/lbf, S_m = 0.0033 rad/lbf, G_s = 0.0117 rad/lbf, and S_s = 0.0033 rad/lbf for small elbow pitch motions. A six-component force-torque sensor was mounted to the end point of each robot for measuring the interaction forces. The control algorithm described above was implemented at a loop rate of 200 Hz.

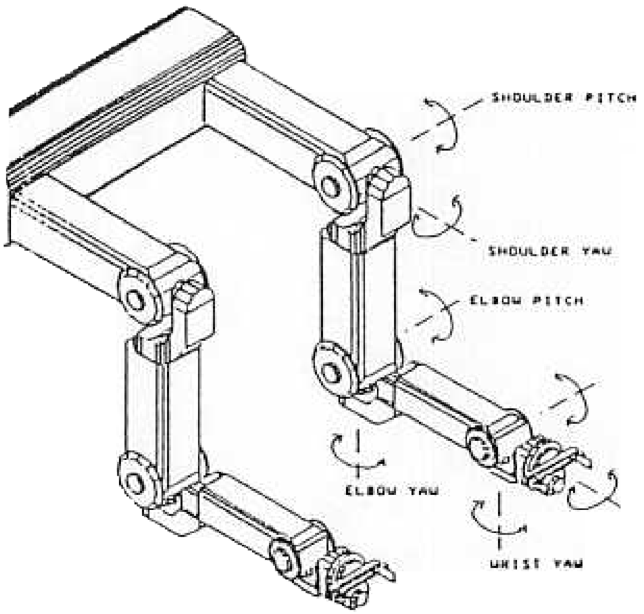

Figure 5: NASA Laboratory Telerobotic Manipulator (slave robot shown)

In the first experiment, the objective was to arbitrarily specify the master impedance for elbow pitch in unconstrained motion. The master impedance was chosen to be Z_m = 100 lbf/rad. The constant value for the master impedance leads to a spring-like behavior for the master arm: the robot's position is directly proportional to the applied force. This causes the robot to return to its initial position after force is removed. However, the human must always work against the restoring force of the spring. Using equations 27 and 12, H_{11} was calculated to be 0.57. An increasing vertical force was exerted on the end of the master robot. The end-point force and the elbow pitch position of the robot were recorded during the maneuver. Figure 6 shows a plot of master force versus master position. The slope of this curve is Z_m; it was calculated with a least-squares curve fit. The measured impedance was Z_m = 101.2 lbf/rad which agrees with the theoretical prediction.

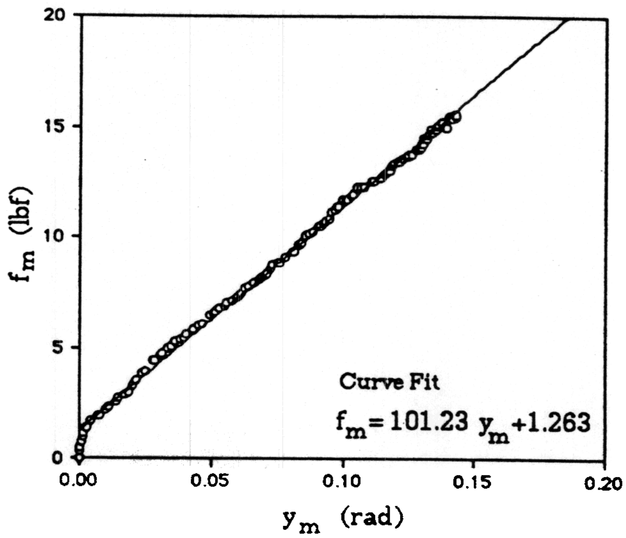

Figure 6: Master robot force vs master robot position; the slope of 101.2 lbf/rad represents the master robot impedance.

In the second experiment, the objective was to shape the master impedance as a damper, such that Z_m = 1 s lbf/rad where s is the Laplace operator. This behavior makes the master robot move with a velocity proportional to the imposed force. The robot force and position were recorded during a elbow pitch maneuver. Figure 7 is a plot of the master force versus master position. There is an initial transient behavior where the force builds up enough to overcome the robot's inertia. Then the curve is fairly flat, indicating that a constant damping force is acting on the robot. After force is removed, the robot will remain in its last position. Since there are no restoring forces acting on the human arm, a damping impedance is the most natural mode of motion for teleoperation.

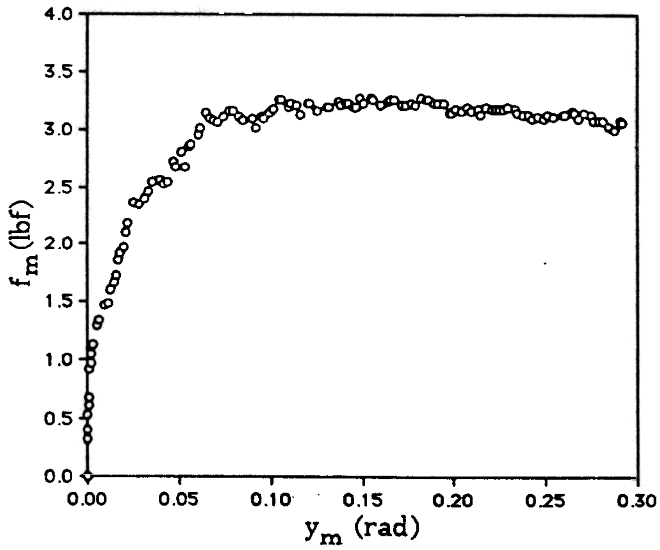

Figure 7: Master robot force vs master robot position; the flat part indicats that the master velocity is proportional to the master force.

The third experiment demonstrates the system behavior when two performance parameters (force ratio and position ratio as given by equations 5 and 6) are specified simultaneously: $R_f = 2$, and $R_y = 1$. The first performance specification states that the force exerted by the slave robot should be twice the force applied to the master robot. The second performance specification implies that the positions of both robots must be identical. A spring scale was employed as a compliant environment with linear stiffness such that E = 217.0 lbf/rad. To satisfy the requirements of system stability, one must guarantee that $Z_s > E$ (inequality 24). Therefore Z_s was chosen to be 223 lbf/rad. Note that, once Z_s, R_f and R_y are chosen, we have no freedom in choosing Z_m. P_{11} was chosen arbitrarily as 0.015 and then equations (8), (9), and (11) were solved for the three remaining unknown elements P_{12}, P_{21}, and P_{22}. Using equations 12, through 15, the H matrix can be found such that:

$$H = \begin{bmatrix} H_{11}=1 & H_{12}=0.25 \\ H_{21}=1.55 & H_{22}=0.10 \end{bmatrix} \qquad (29)$$

The master robot was moved through a series of elbow pitch motions by the human operator. The end-point forces and joint positions of both robots were recorded during the maneuver. The robot forces are plotted versus time in Figure 8. The slave force varies in phase with the master force as the spring scale is alternately compressed and released. The amplitude of the slave force is double the amplitude of the master force. The force ratio can be determined from Figure 9, which is a plot of slave force versus master force. A least-squares curve fit yields a slope of $R_f = 2.02$. The robot positions are plotted versus time in Figure 10. The slave robot tracks the master robot closely. The measured position ratio is $R_y = 0.98$. The actual values of the force ratio and the position ratio agree well with their specified values.

The purpose of placing the performance criterion on the slave impedance was to guarantee stability of the telerobotic system during the experiment. However, it was not possible to measure the magnitude of Z_s because the slave robot was constrained by the environment. The only conclusion that can be inferred is that the slave impedance was greater than the impedance of the environment. Otherwise, the system would have been unstable. It will be shown that this must be true in the next series of experiments.

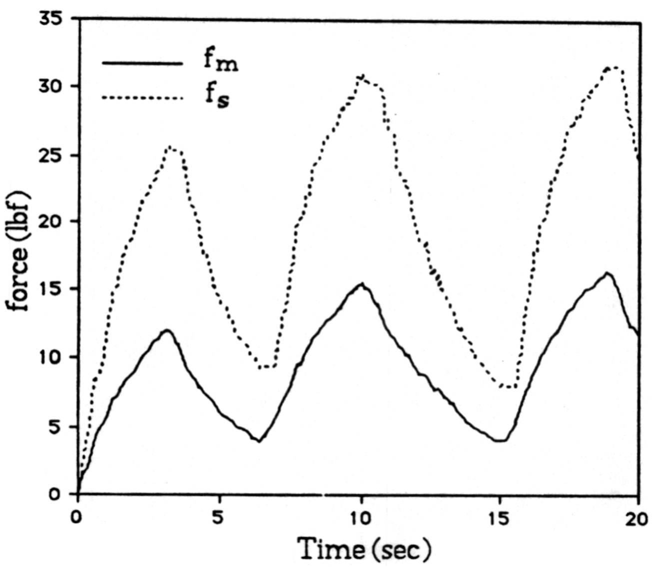

Figure 8: The slave robot force is more than the master robot force by factor of two

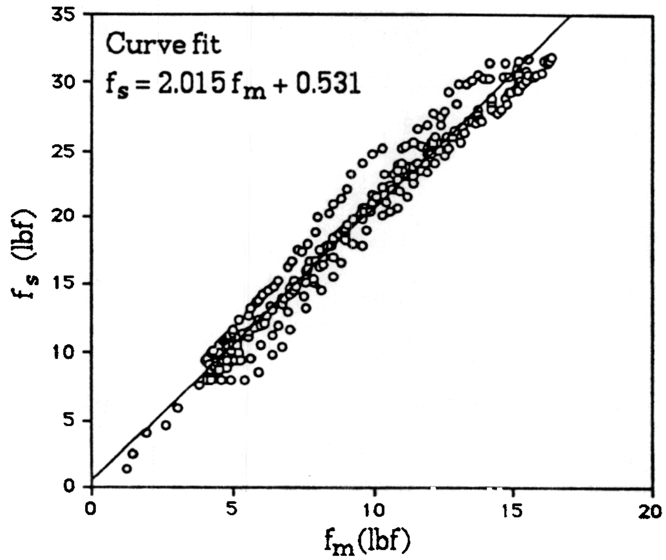

Figure 9: Slave robot force vs the master robot force; $R_f = 2$

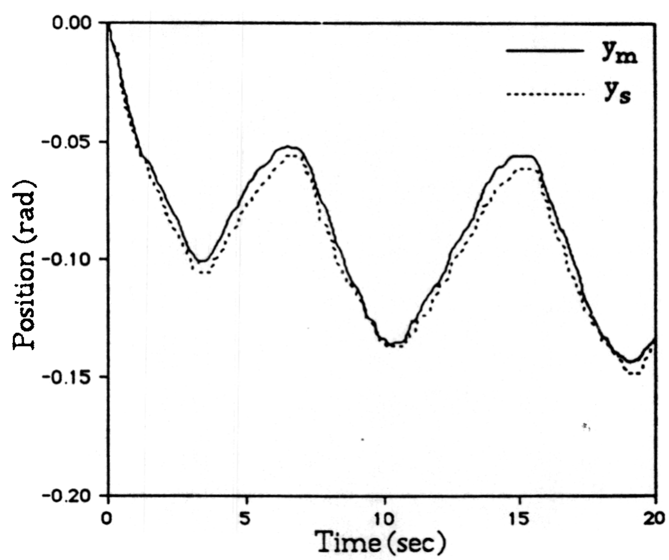

Figure 10: The slave robot tracks the master robot closely.

In the fourth experiment, the objective was to verify the sufficiency of the stability condition for constrained motion. Inequality (24) is a sufficient but not a necessary condition for stability of the slave robot. In other words, the robot may be stable if $|Z_s| < |E|$, but it can never be unstable if $|Z_s| > |E|$.

Z_s was chosen to be equal to E satisfying the stability condition 24. The slave robot compressed a spring scale that simulated a compliant environment. The reaction force on the slave robot was recorded during the maneuver. Figure 11 shows that the system is stable when interacting with the spring. Next the slave impedance was set to 0.5E. The slave force oscillates violently, indicating that the slave robot is unstable. The results are shown in Figure 12. It verified that inequality 24 is violated when unstable contact, as indicated by the unbounded contact force, occurs. It can be concluded from the previous two experiments that the transition from stable to unstable behavior occurs somewhere in the region \.5E < Z_s < E.

The stability condition for unconstrained motion (inequality 26) can be verified in a similar manner. A lower bound for stability is established on the master robot impedance, Z_m. It can be shown that this lower bound is no greater than the human arm impedance, S_h.

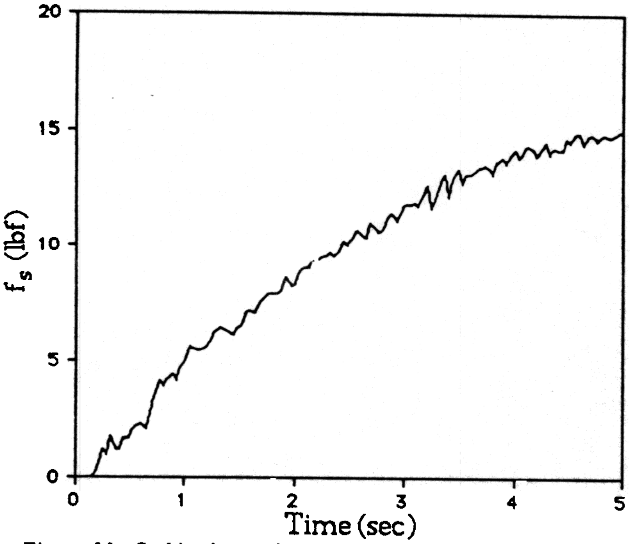

Figure 11: Stable slave robot force. Z_s satisfies inequality 24.

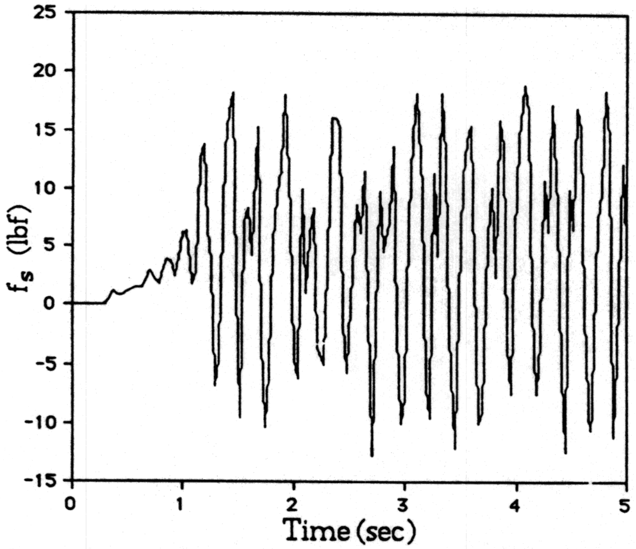

Figure 12: Unstable master robot force. Zs violates inequality 24.

Conclusions

The bilateral impedance control architecture differs from previous approaches in that force signals travel in both directions between the master and slave robots. The communication of force signals within the system is regulated by the H matrix. By tailoring the structure of the H matrix, it is possible to arbitrarily specify desired system performance characteristics. This is the primary advantage of bilateral impedance control.

System performance can be completely described by a set of three independent parameters. These parameters may be the force ratio, the position ratio, or the impedance of either robot. To form an independent set, one of the parameters must be the slave impedance. The performance parameters are functions of the system variables that govern the dynamic behavior of the robots, the human arm, and the environment. In addition, the performance parameters are fundamentally related to the elements in the H matrix. By selecting the relative magnitudes of these four elements, three performance parameters can be specified simultaneously.

The only limitations on the choice of performance parameters are imposed by the requirements for system stability. There are two conditions that are sufficient to guarantee stability. For unconstrained motion, the master impedance must be greater than the impedance of the human arm. For constrained motion, the slave impedance must be greater than the impedance of the environment. Since both the master and slave impedances are performance parameters that can be arbitrarily specified, it is not necessary to trade off performance and stability in most cases.

References

1. Anderson, R. J., *A Network Approach to Force Control in Robotics and Teleoperation*, Ph. D. Thesis, University of Illinois, January 1989.
2. Hannaford, B., "A Design Framework for Teleoperators with Kinesthetic Feedback," *IEEE Transactions on Robotics and Automation*, Vol. 5, No. 4, August 1989.
3. Jansen, J. F., and Herndon, J. N., "Design of a Telerobotic Controller with Joint Torque Sensors," in *Proceedings of the IEEE International Conference on Robotics and Automation*, 1990.
4. Raju, G. J., Verghese, G. C., and Sheridan, T. B., "Design Issues in 2-port Network Models of Bilateral Remote Manipulation," in *Proceedings of the IEEE International Conference on Robotics and Automation*, 1989.
5. Moore, C. L., *Performance and Stability of Telemanipulators Using Bilateral Impedance Control*, Ph. D. Thesis, University of Minnesota, December 1991.
6. Kazerooni, H., "Human-Robot Interaction via the Transfer of Power and Information Signals," *IEEE Transactions on Systems, Man, and Cybernetics*, Vol. 20, No. 2, March 1990.
7. Kazerooni, H., Tsay, T. I., and Moore, C. L., "Telefunctioning: An Approach to Telerobotic Manipulations," American Control Conference, San Diego, CA, May 1990.
8. Lehtomaki, N. A., Sandell, N. R., and Athans, M., "Robustness Results in Linear-Quadratic Gaussian Based Multivariable Control Designs," *IEEE Transactions on Automatic Control*, Vol. 26, No. 1, pp. 75-92, February 1981.
9. Craig, J. J., *Introduction to Robotics; Mechanics and Control*, Addison-Wesley Publishing Company, 1988.
10. Herndon, J. N., Babcock, S. M., Butler, P. L., Costello, H. M., Glassell, R. L., Kress, R. L., Kuban, D. P., Rowe, J. C., Williams, D. M., and Meintel, A. J., "Telerobotic Manipulator Developments for Ground-Based Space Research," ANS Meeting on Robotics and Remote Systems, Charleston, SC, March 1989.
11. Barker, L. K., and McKinney, Jr., W. S., "Optimized Resolved Rate Control of Seven- Degree-of-Freedom Laboratory Telerobotic Manipulator (LTM) with Application to Three-Dimensional Graphics Simulation," NASA Technical Paper 2938, October 1989.
12. Tsay, T. I., Kazerooni, H., "A Design Framework for Telerobotics using the H_∞ Approach", American Control Conference, Chicago, Il 1992.